Measurements of the CP structure of Higgs boson couplings with the ATLAS detector

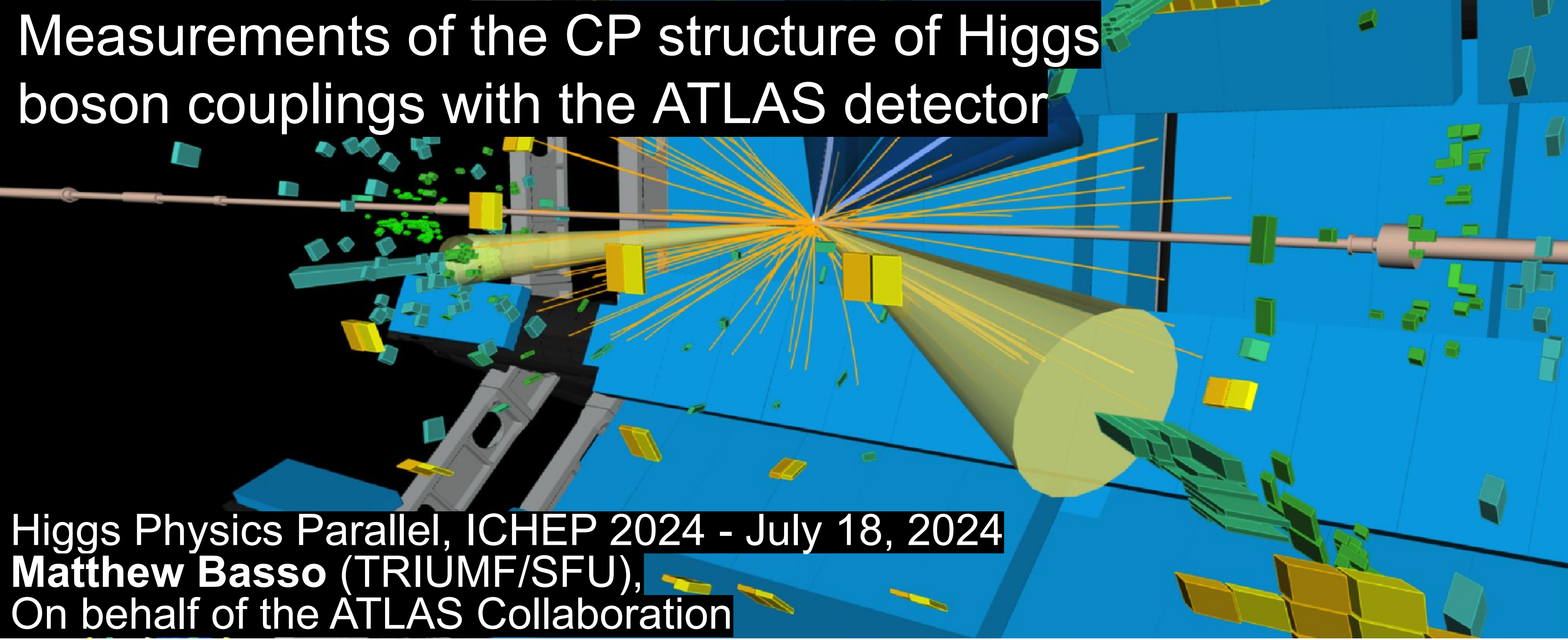

Higgs Physics Parallel, ICHEP 2024 - July 18, 2024

Matthew Basso (TRIUMF/SFU),
On behalf of the ATLAS Collaboration

ICHEP 2024
PRAGUE
ichep2024.org
42nd International Conference on High Energy Physics
18-24 July 2024 · Prague · Czech Republic

ATLAS EXPERIMENT

TRIUMF

SFU SIMON FRASER UNIVERSITY

Source for event display: HIGG-2019-10

https://indico.cern.ch/event/1291157/contributions/5876702/

CP violation and the Higgs boson

- Only known source of CP violation occurs in CKM matrix → **insufficient** to explain baryon asymmetry in the Universe
- SM Higgs is predicted to be CP-even
  - While CP-odd-only couplings have strongly excluded by ATLAS and CMS, **CP-even/odd mixing has not**
- Recent ATLAS measurements studying Higgs CP properties using 139 fb^{-1} at $\sqrt{s}$ = 13 TeV:
  - VBF, $H\rightarrow\gamma\gamma$: PRL 131 (2023) 061802
  - $H\rightarrow ZZ^*\rightarrow 4\ell$: JHEP 05 (2024) 105
  - VBF, $H\rightarrow WW^*\rightarrow e\nu\mu\nu$: PRD 108 (2023) 072003
  - $H\rightarrow\tau\tau$: EPJC 83 (2023) 563
  - ttH+tH, $H\rightarrow bb$: PLB 849 (2024) 138469

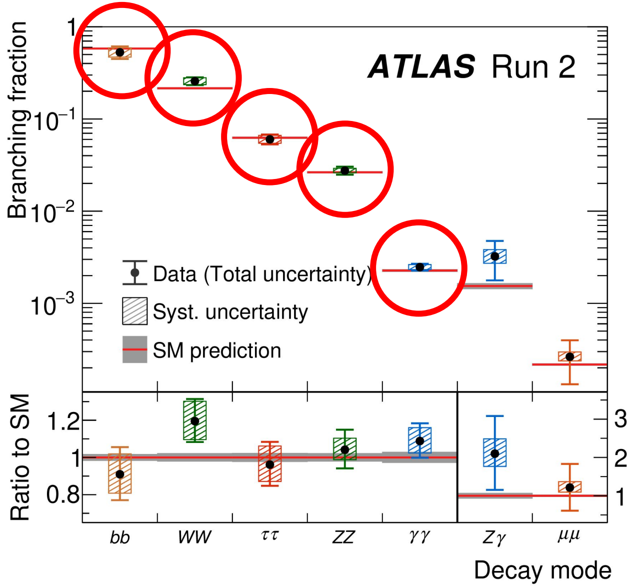

Nature 607 (2022) 52

Let's review them!

Higgs production and decay diagrams

Gluon-gluon fusion (ggF)

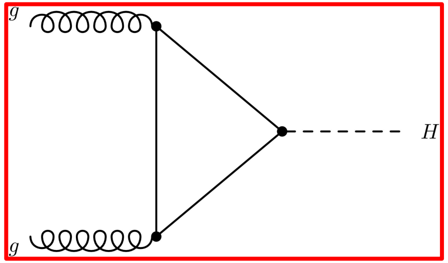

Vector boson fusion (VBF)

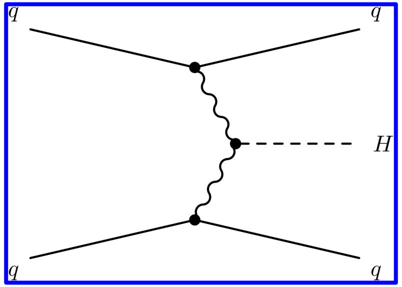

Associated production (*VH*)

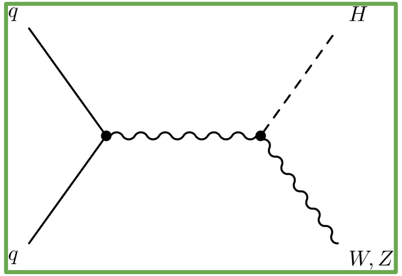

JHEP 08 (2016) 045

ttH* and *tH

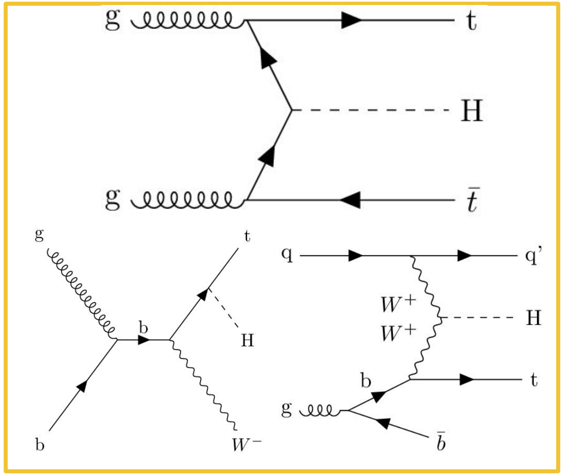

PLB 849 (2024) 138469

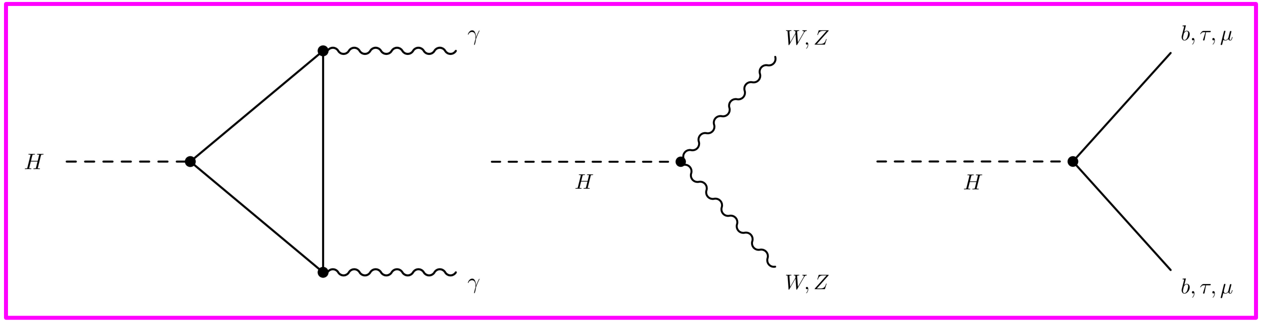

Decays to photons, vector bosons, and fermions

CP-odd models and signal morphing

- Higgs→bosons measurements: add dim-6 CP-odd operators in an effective field theory to the SM Lagrangian and measure their couplings *c* (= 0 in SM):

$$|\mathcal{M}|^2 = \left|\mathcal{M}_{\rm SM} + \sum_i \frac{c_i}{\Lambda^2}\mathcal{M}_{{\rm BSM},i}\right|^2$$
$$= |\mathcal{M}_{\rm SM}|^2 + 2\sum_i \frac{c_i}{\Lambda^2}\Re\left(\mathcal{M}^*_{\rm SM}\mathcal{M}_{{\rm BSM},i}\right) + \sum_i\sum_j \frac{c_i c_j}{\Lambda^4}\Re\left(\mathcal{M}^*_{{\rm BSM},i}\mathcal{M}_{{\rm BSM},j}\right)$$

CP-even (→ $|\mathcal{M}_{\rm SM}|^2$)
CP-odd (→ interference term)
CP-even (→ quadratic term)

  - Effect on Higgs signal introduced via reweighting using MadGraph+SMEFTsim for a particular choice of operator basis (e.g., Warsaw, Higgs, HISZ, …) and morphing using couplings *c*
- Higgs→fermions measurements: CP-odd mixing may occur in Yukawa couplings at tree level and can be introduced via an effective term:

$$\mathcal{L}_{H\tau\tau} = -\frac{m_\tau}{v}\kappa_\tau(\cos\phi_\tau\bar{\tau}\tau + \sin\phi_\tau\bar{\tau}i\gamma_5\tau)H,$$

  - Higgs signal can be morphed between different scenarios by tuning Yukawa coupling κ (= 1 in SM) and CP mixing angle ϕ (= 0 in SM)

CP-sensitive observables

- CP properties of the Higgs are extracted via fits to CP-sensitive observables
  - CP mixing leads to **asymmetric distributions** in sensitive observables (as opposed to symmetric in SM)
- Optimal Observable (OO) is one such observable:

$$\mathcal{OO} = \frac{2\Re\left(\mathcal{M}^*_{\mathrm{SM}}\mathcal{M}_{\mathrm{BSM}}\right)}{|\mathcal{M}_{\mathrm{SM}}|^2}.$$

  - By construction, it is CP-odd
  - Shape is insensitive to the inclusion of terms quadratic in couplings *c* → **probes genuine CP-violating effects**

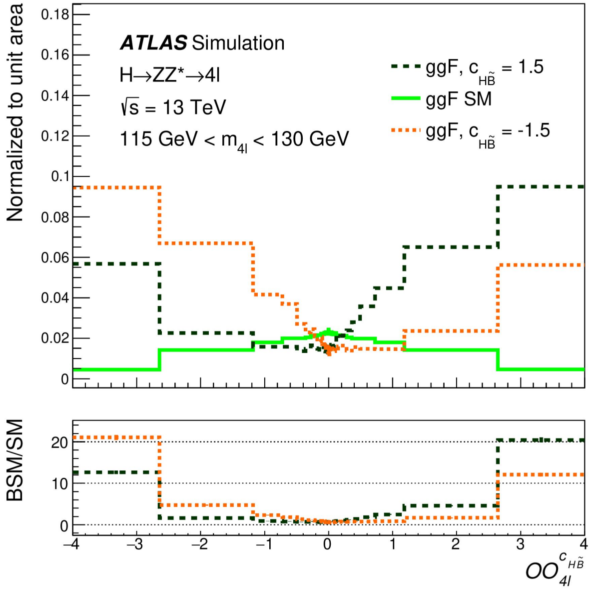

JHEP 05 (2024) 105

VBF, $H \to \gamma\gamma$

[PRL 131 (2023) 061802]

- Use boosted decision trees (BDTs) to separate VBF from ggF and then VBF from continuum $\gamma\gamma$ background
  - Use CP-even dijet and diphoton variables as inputs to both BDTs
  - Specifically targets the VBF production vertex
- Events are split into signal regions (SRs) using BDT scores and further split according to OO
  - Calculated from 4-momenta of Higgs candidate and dijet system

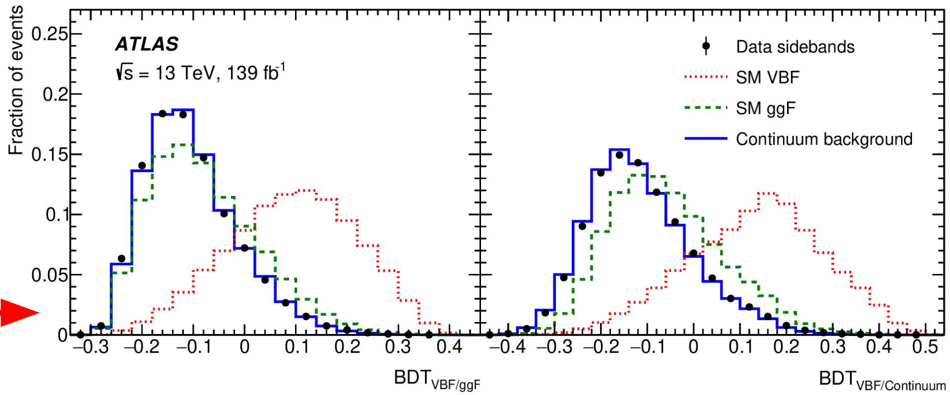

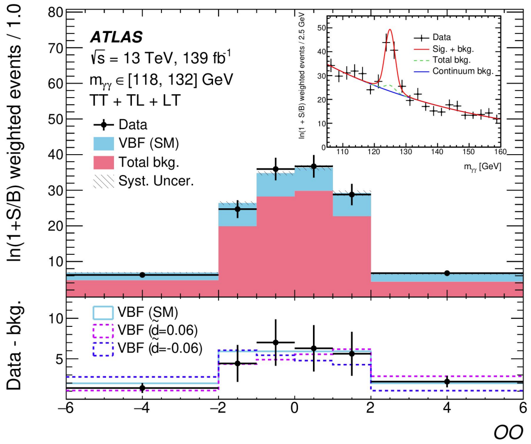

VBF, $H \to \gamma\gamma$

- Unbinned fit to $\gamma\gamma$ invariant mass spectrum performed in each OO bin
  - Signal normalization is floated by an additional parameter → **only shape in OO is exploited**
- Consider scenarios with CP-odd modifications to Higgs-boson couplings:
  - $\tilde{d}$ in [−0.034; 0.071] @ 95% CL (HISZ basis)
  - $c_{H\tilde{W}}$ in [−0.55, 1.07] @ 95% CL (Warsaw basis)
- Results are compatible with the SM expectation: **no CP violation is observed**

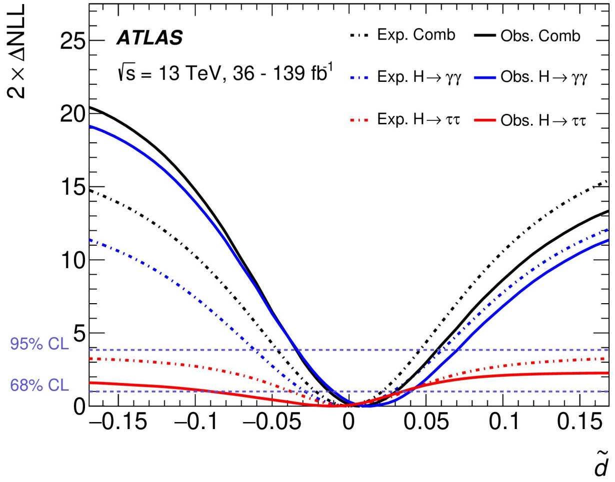

PRL 131 (2023) 061802

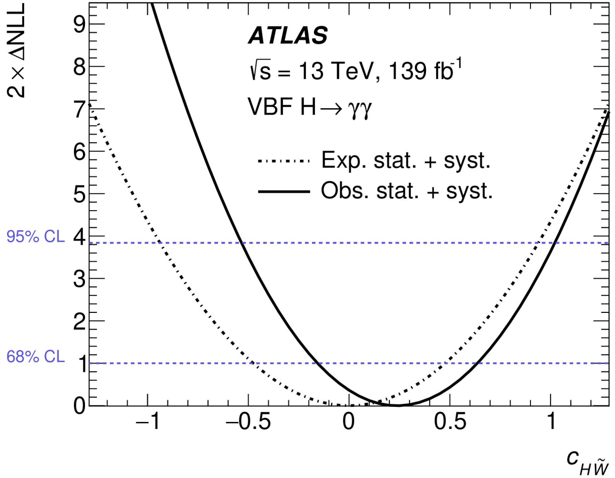

$H \to ZZ^* \to 4\ell$

- Consider $4e$, 4μ, and $2e2\mu$ final states
  - SRs constructed according to 4-lepton invariant mass, jet multiplicity, dijet invariant mass, and VBF deep neural network (DNN) score (4 bins)
- Construct an OO for each dim-6 CP-odd operator
  - Consider Warsaw, Higgs, and HISZ basis operators affecting Higgs-boson couplings
  - Build OOs for production-only (VBF+VH), decay-only (ggF, VBF, VH, ttH, …), and combined effects

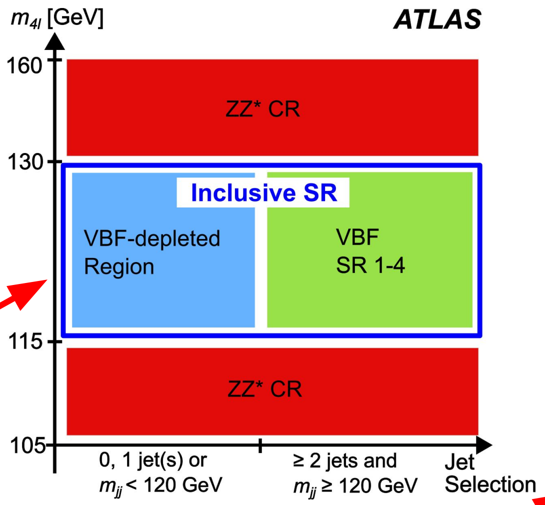

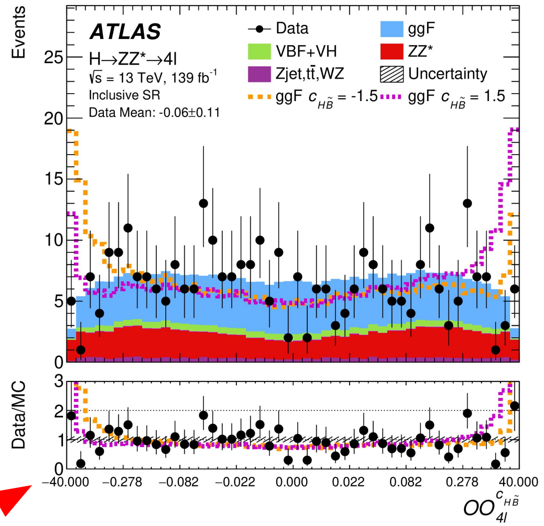

Operator	Structure	Coupling
	Warsaw Basis	
$O_{\Phi\tilde W}$	$\Phi^\dagger\Phi\tilde W^I_{\mu\nu}W^{\mu\nu I}$	$c_{H\widetilde W}$
$O_{\Phi\tilde W B}$	$\Phi^\dagger\tau^I\Phi\tilde W^I_{\mu\nu}B^{\mu\nu}$	$c_{H\widetilde W B}$
$O_{\Phi\tilde B}$	$\Phi^\dagger\Phi\tilde B_{\mu\nu}B^{\mu\nu}$	$c_{H\tilde B}$
	Higgs Basis	
$O_{hZ\tilde Z}$	$hZ_{\mu\nu}\tilde Z^{\mu\nu}$	$\tilde c_{zz}$
$O_{hZ\tilde A}$	$hZ_{\mu\nu}\tilde A^{\mu\nu}$	$\tilde c_{z\gamma}$
$O_{hA\tilde A}$	$hA_{\mu\nu}\tilde A^{\mu\nu}$	$\tilde c_{\gamma\gamma}$

JHEP 05 (2024) 105

$H \to ZZ^* \to 4\ell$

- Perform simultaneous fit to OO distributions, considering **only OO shape** in each region
- Also **unfold OOs to particle level** → sensitive to BSM effects on **both shape and rate**
- Couplings results and differential measurements indicate **no CP asymmetry**

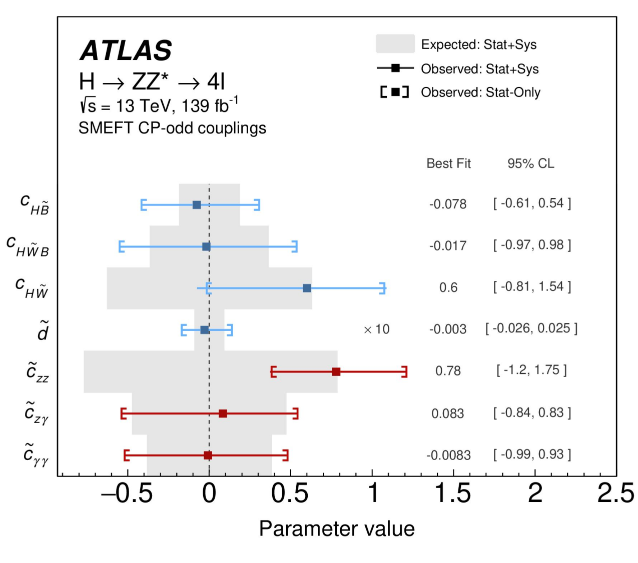

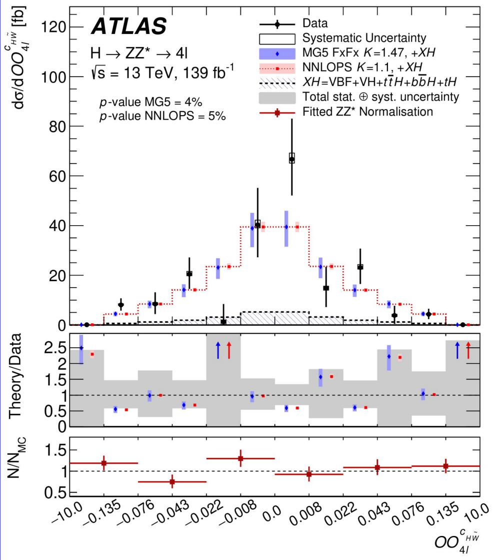

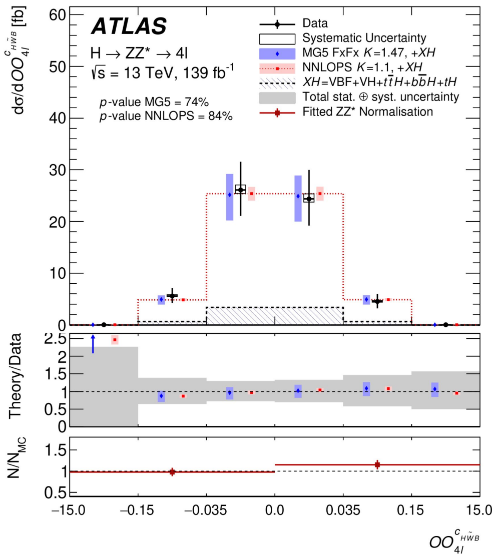

JHEP 05 (2024) 105

VBF, $H \to WW^* \to e\nu\mu\nu$

$$\Delta\phi_{jj}^{\text{signed}} = \begin{cases} \phi_{j_0} - \phi_{j_1} & \eta_{j_0} > \eta_{j_1} \\ \phi_{j_1} - \phi_{j_0} & \eta_{j_1} > \eta_{j_0} \end{cases},$$

- Employ a combination of BDTs targeting VBF, ggF, and top+VV production to produce regions enriched in VBF
  - Detector-level signal in different variables extracted via multi-bin fit and **unfolded to particle level**
- **Signed dijet azimuthal separation $\Delta\phi_{jj}$** is sensitive to CP-odd effects
  - Consider effects on production+decay from dim-6 CP-odd operators to unfolded $\Delta\phi_{jj}$
- Constraints measured for several effective Higgs-boson couplings ($c_{HW\sim}$, $c_{HB\sim}$, and $c_{HWB\sim}$) $\to$ **no CP violation observed**

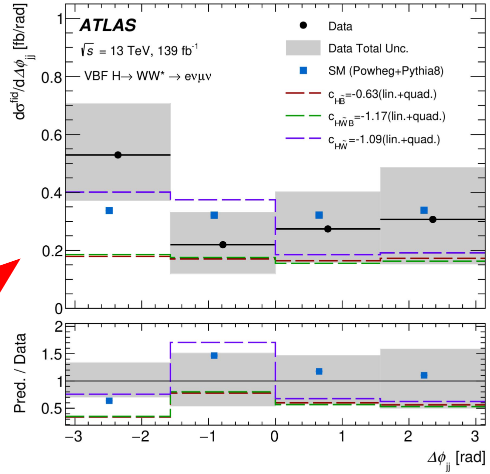

PRD 108 (2023) 072003

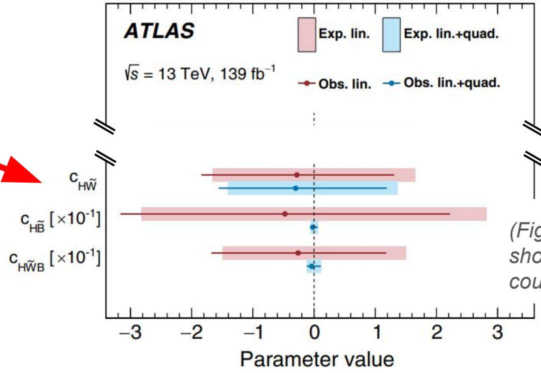

(Figure cropped to show only CP-odd couplings)

$H \rightarrow \tau\tau$

$H \rightarrow \tau^{+}\tau^{+} \rightarrow \pi^{+}\pi^{-}\nu\nu$

- Consider semileptonic ($\tau_{\mathrm{lep}}\tau_{\mathrm{had}}$) and hadronic ($\tau_{\mathrm{had}}\tau_{\mathrm{had}}$) decay channels
  - τ_{had} decays are then subdivided according to number of charged and neutral pions
- SRs defined using tau and jet kinematics and VBF BDT score
  - Lepton impact parameters and tau spin analyzing functions split SRs into regions of different sensitivity
- Signed acoplanarity angle ϕ^{*}_{CP} between the tau decay planes sensitive to CP mixing angle ϕ_{τ}

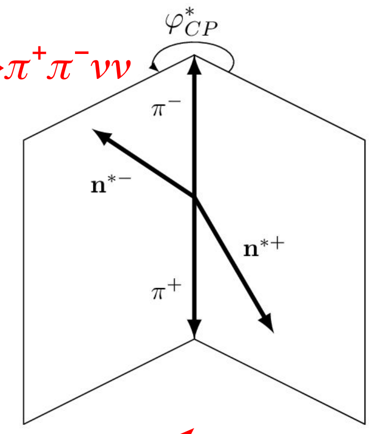

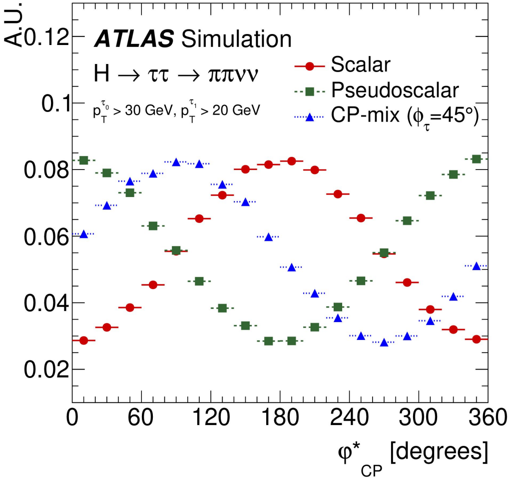

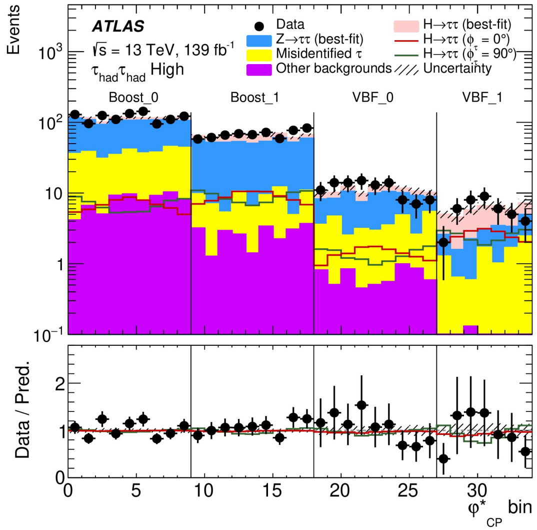

EPJC 83 (2023) 563

$H \to \tau\tau$

- Simultaneous fit floats tau Yukawa coupling μ_τ → **only shape in ϕ^*_{CP}** is used in discerning CP-odd effects
- Observe **ϕ_τ = 9 ± 16° @ 68% CL** → ***exclude*** pure CP-odd scenario (ϕ_τ = 90°) at **3.4σ level**

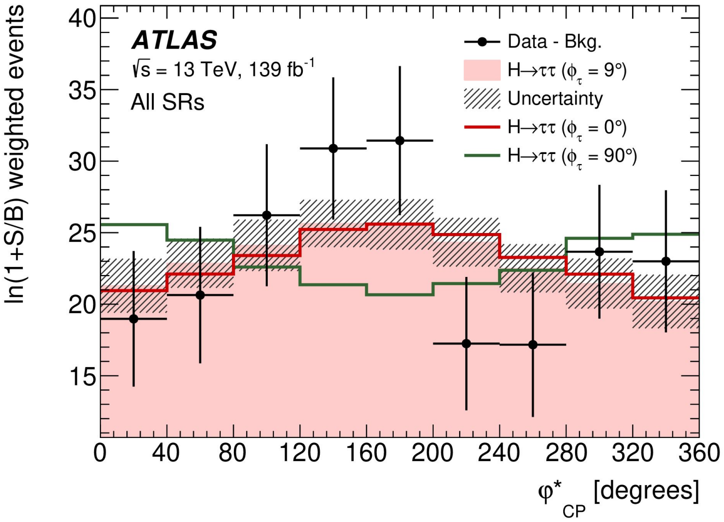

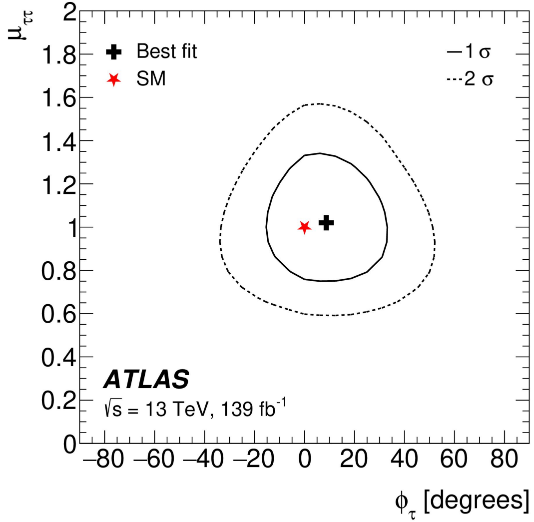

EPJC 83 (2023) 563

ICHEP 2024

ttH+tH, $H\rightarrow bb$

- Analysis split into ℓ+jets and dilepton categories
  - Further subdivided according to the number of jets, number of *b*-jets, and boosted signatures
- BDTs trained for various purposes:
  - Reconstruction: assigns jets from Higgs or top quark decays
  - Classification: separates *ttH* from background
- CP sensitive observables:

$$b_2 = \frac{(\vec{p}_1 \times \hat{z}) \cdot (\vec{p}_2 \times \hat{z})}{|\vec{p}_1||\vec{p}_2|}, \quad \text{and} \quad b_4 = \frac{(\vec{p}_1 \cdot \hat{z})(\vec{p}_2 \cdot \hat{z})}{|\vec{p}_1||\vec{p}_2|},$$

  - $\mathbf{p}_{1/2}$ ≔ top quark momenta, $\mathbf{z}$ ≔ beam axis
  - Assumes knowledge of neutrino 4-momenta to reconstruct $\mathbf{p}_{1/2}$ → using neutrino weighting for dilepton events

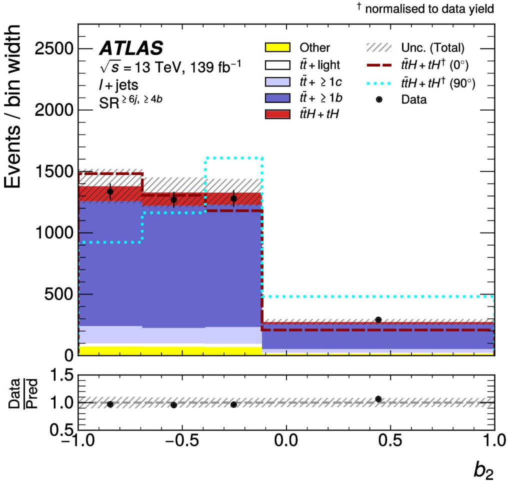

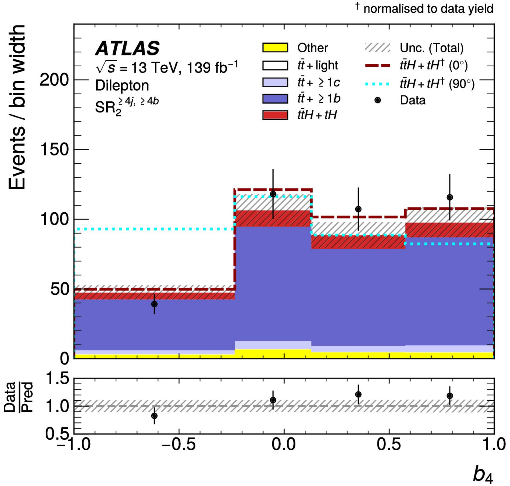

PLB 849 (2024) 138469

ttH+tH, H→bb

PLB 849 (2024) 138469

- Destructive interference between diagrams with *H-t* and *H-W* couplings leads to small *tH* signal → analysis optimized for *ttH*
  - Couplings separately treated in the CP-even/odd parameterization and lead to sizable modifications to the *tH*:*ttH* cross section ratio
- *H-t* Yukawa coupling κ_t also floats in fit
  - Only shape is exploited
- Observed value of CP mixing angle: $\alpha = 11^{\circ}{}^{+52^{\circ}}_{-73^{\circ}}$
  - ***Exclude*** pure CP-odd scenario (α = 90°) at **1.2σ level**

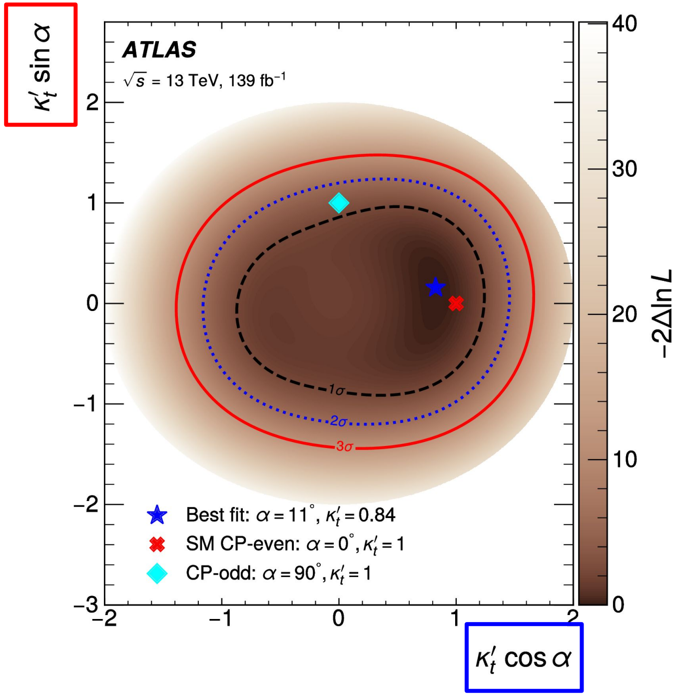

$$\mathcal{L}_{t\bar{t}H} = -\kappa_t' y_t \phi \bar{\psi}_t (\cos\alpha + i\gamma_5 \sin\alpha)\psi_t \, ,$$

Summary

- Presented ATLAS's recent measurement program studying the CP structure of the Higgs
  - Observed results are consistent with a CP-even Higgs → **no CP-violation has been observed**
- For nearly all of the measurements described, the precision is limited by the **availability of data → LHC Run 3 data will improve the study of CP-violating effects in the Higgs sector**
  - Going from Run 2 → Run 2+3 will **improve** the statistical precision by √**3 ~ 1.7×**
  - *ttH*+*tH*, *H*→*bb* measurement limited by systematic uncertainties

Source

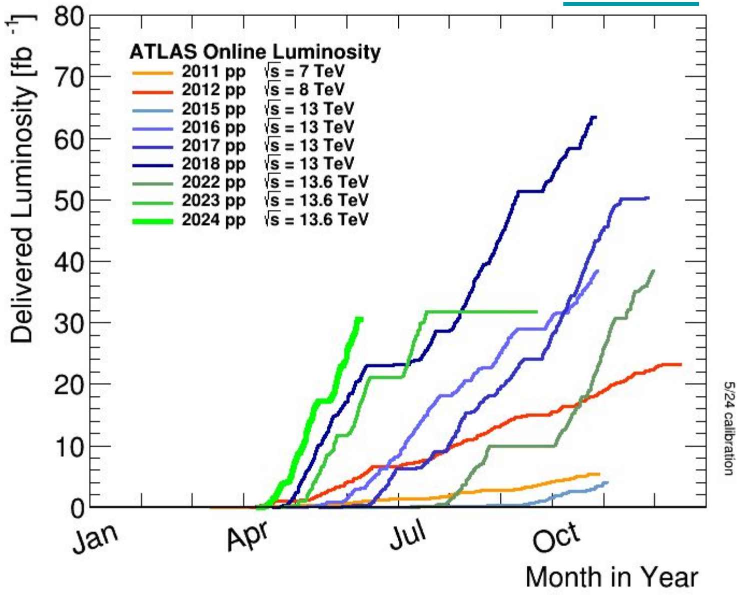

Also see C. Young's talk tomorrow on the latest measurements of $H \to \tau\tau$ properties using ATLAS, including new CP studies of those properties!

Source: ATLAS-CONF-2019-025

Thank you for listening!
Questions?

Source: HIGG-2021-20

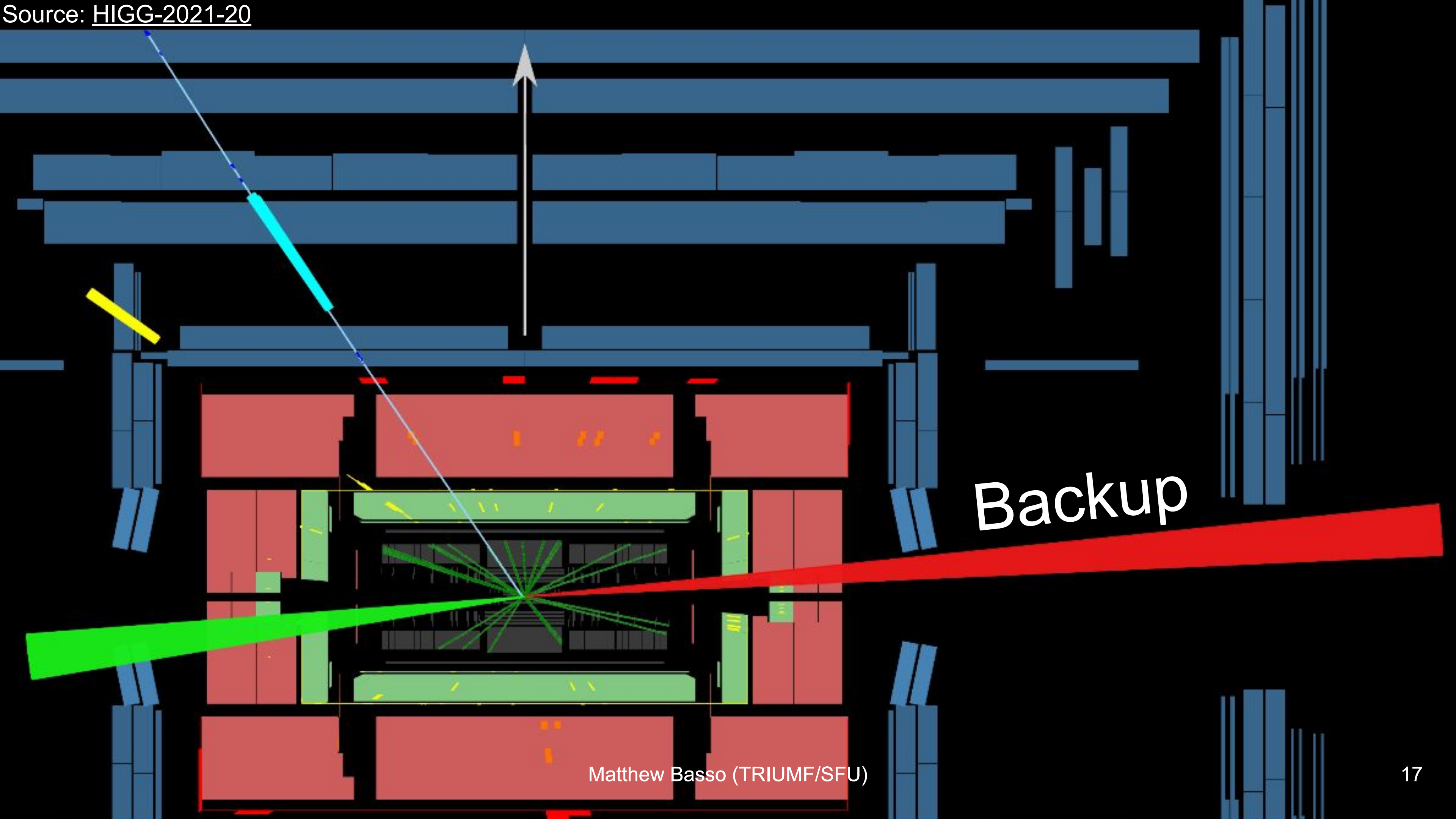

Backup

VBF, $H\to\gamma\gamma$: miscellaneous

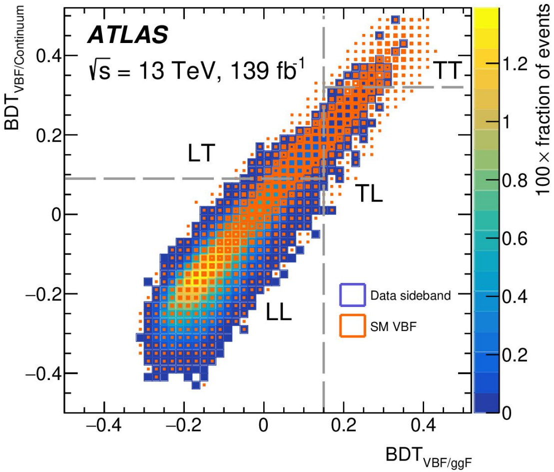

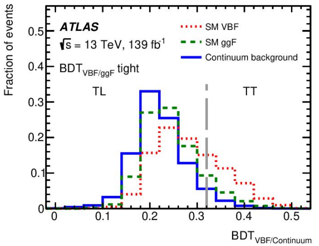

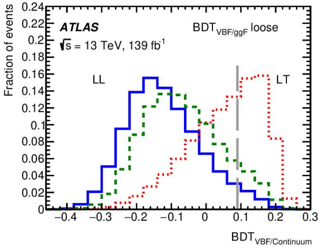

[PRL 131 (2023) 061802]

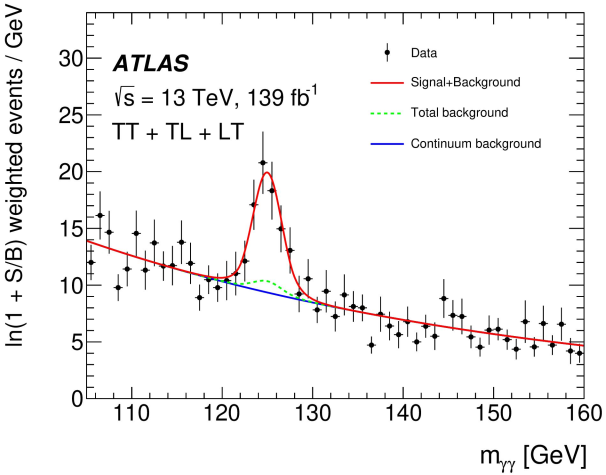

$\gamma\gamma$ invariant mass spectrum among all signal regions

Table 1: Observed and expected 68% and 95% confidence intervals for $\tilde{d}$ and $c_{H\tilde{W}}$. Results for scenarios with the interference-only (noted as 'inter. only') term and interference-plus-quadratic terms (noted as 'inter.+quad.') are both presented. Combined results for $\tilde{d}$ including the $H\to\tau\tau$ analysis are shown. The expected results of $H\to\tau\tau$ are slightly different from Ref. due to the different correlation scheme between their signal region and control region.

	68% (exp.)	95% (exp.)	68% (obs.)	95% (obs.)
$\tilde{d}$ (inter. only)	[−0.027, 0.027]	[−0.055, 0.055]	[−0.011, 0.036]	[−0.032, 0.059]
$\tilde{d}$ (inter.+quad.)	[−0.028, 0.028]	[−0.061, 0.060]	[−0.010, 0.040]	[−0.034, 0.071]
$\tilde{d}$ from $H\to\tau\tau$	[−0.038, 0.036]	–	[−0.090, 0.035]	-
Combined $\tilde{d}$	[−0.022, 0.021]	[−0.046, 0.045]	[−0.012, 0.030]	[−0.034, 0.057]
$c_{H\tilde{W}}$ (inter. only)	[−0.48, 0.48]	[−0.94, 0.94]	[−0.16, 0.64]	[−0.53, 1.02]
$c_{H\tilde{W}}$ (inter.+quad.)	[−0.48, 0.48]	[−0.95, 0.95]	[−0.15, 0.67]	[−0.55, 1.07]

$H\to ZZ^*\to 4\ell$: composition and post-fit yields

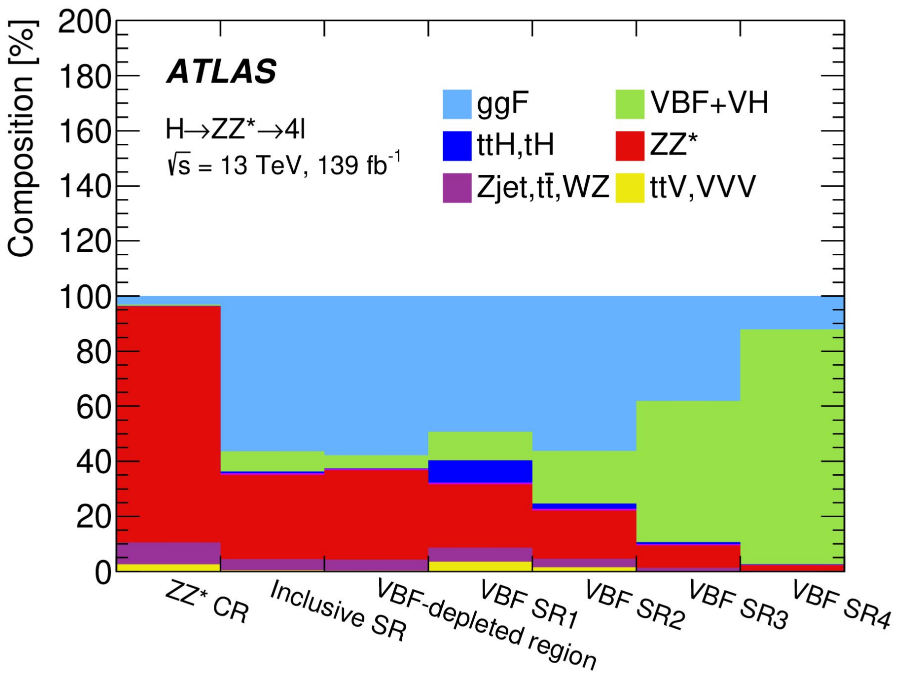

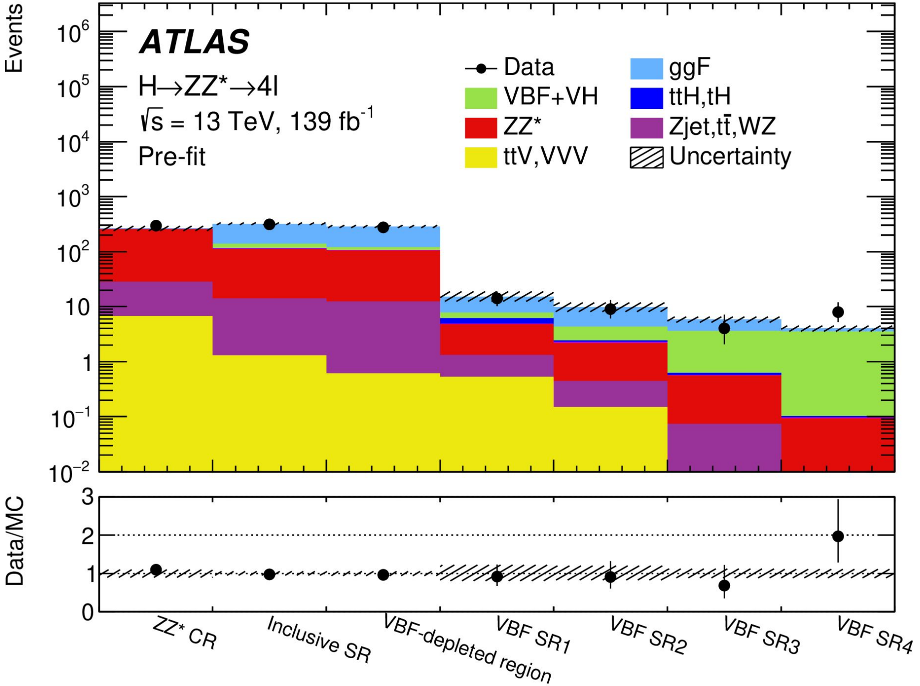

[JHEP 05 (2024) 105]

$H \to ZZ^* \to 4\ell$: fiducial space space

Leptons and jets	
Leptons	$p_T > 5$ GeV, $\|\eta\| < 2.7$
Jets	$p_T > 30$ GeV, $\|y\| < 4.4$
Lepton selection and pairing	
Lepton kinematics	$p_T > 20, 15, 10$ GeV
Leading pair (m_{12})	SFOC lepton pair with smallest $\|m_Z - m_{\ell\ell}\|$
Subleading pair (m_{34})	Remaining SFOC lepton pair with smallest $\|m_Z - m_{\ell\ell}\|$
Event selection (at most one quadruplet per event)	
Mass requirements	50 GeV $< m_{12} <$ 106 GeV and $m_{\text{threshold}} < m_{34} <$ 115 GeV
Lepton separation	$\Delta R(\ell_i, \ell_j) > 0.1$
Lepton/Jet separation	$\Delta R(\ell_i, \text{jet}) > 0.1$
J/ψ veto	$m(\ell_i, \ell_j) > 5$ GeV for all SFOC lepton pairs
Mass window	105 GeV $< m_{4\ell} <$ 160 GeV
If an extra lepton with $p_T > 12$ GeV is found, the quadruplet with the largest squared matrix element value is kept	

JHEP 05 (2024) 105

$H \rightarrow ZZ^* \rightarrow 4\ell$: constraints on dim-6 operators

JHEP 05 (2024) 105

EFT coupling parameter	Expected 68% CL	Expected 95% CL	Observed 68% CL	Observed 95% CL	Best-fit value	SM p-value	Fit type
$c_{H\tilde{B}}$	[−0.18, 0.19]	[−0.37, 0.37]	[−0.42, 0.31]	[−0.61, 0.54]	−0.078	0.86	decay
$c_{H\tilde{W}B}$	[−0.36, 0.36]	[−0.72, 0.72]	[−0.56, 0.53]	[−0.97, 0.98]	−0.017	0.99	decay
$c_{H\tilde{W}}$	[−0.63, 0.63]	[−1.26, 1.28]	[−0.07, 1.09]	[−0.81, 1.54]	0.60	0.37	comb
$\tilde{d}$	[−0.009, 0.009]	[−0.018, 0.018]	[−0.017, 0.014]	[−0.026, 0.025]	−0.003	0.86	decay
$\tilde{c}_{zz}$	[−0.77, 0.79]	[−2.4, 2.4]	[0.37, 1.21]	[−1.20, 1.75]	0.78	0.11	prod
$\tilde{c}_{z\gamma}$	[−0.47, 0.47]	[−0.76, 0.76]	[−0.54, 0.54]	[−0.84, 0.83]	0.083	0.93	decay
$\tilde{c}_{\gamma\gamma}$	[−0.38, 0.38]	[−0.76, 0.77]	[−0.52, 0.48]	[−0.99, 0.93]	−0.01	0.99	decay

Only one Wilson coefficient c is floated at time

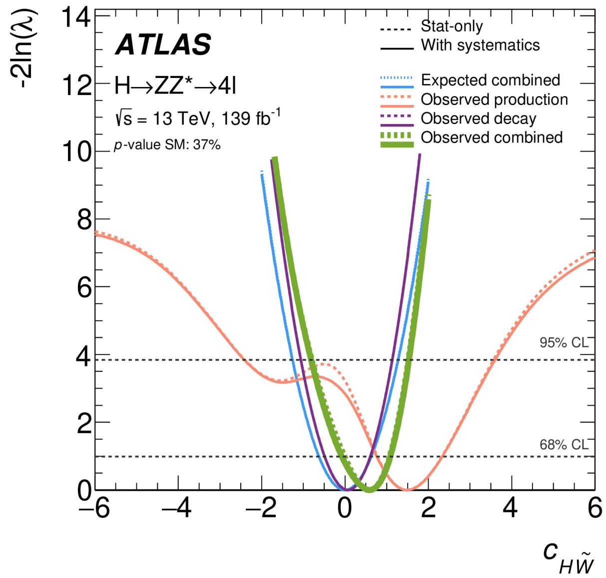

EFT coupling	Expected 95% CL production-only	Expected 95% CL decay-only	Expected 95% CL combined
$c_{H\tilde{B}}$	–	±0.37	–
$c_{H\tilde{W}B}$	–	±0.72	–
$c_{H\tilde{W}}$	±4.8	±1.34	±1.27
$\tilde{d}$	±0.63	±0.018	±0.019
$\tilde{c}_{zz}$	±2.4	–	–
$\tilde{c}_{z\gamma}$	±6.6	±0.76	±0.80
$\tilde{c}_{\gamma\gamma}$	–	±0.76	–

VBF, $H \to WW^* \to e\nu\mu\nu$: regions and post-fit yields

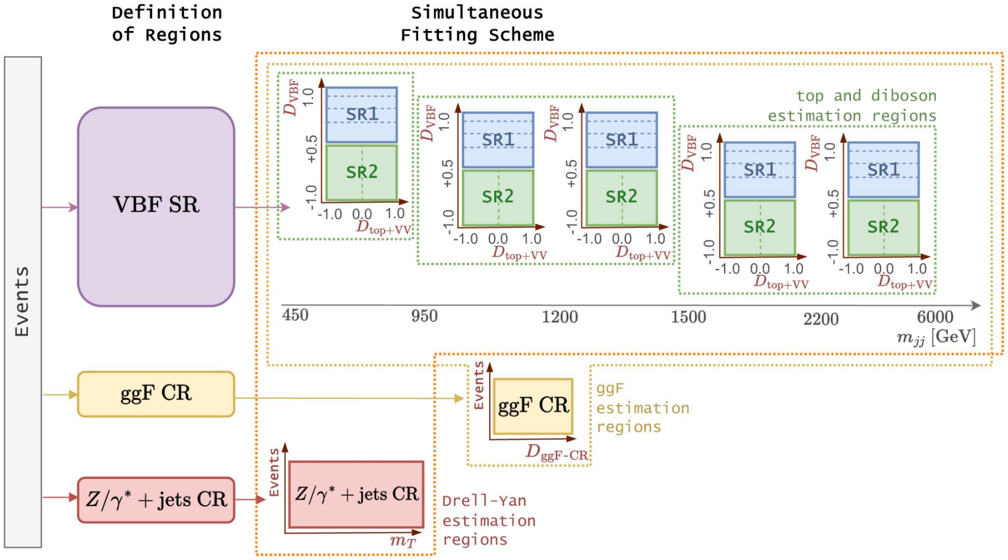

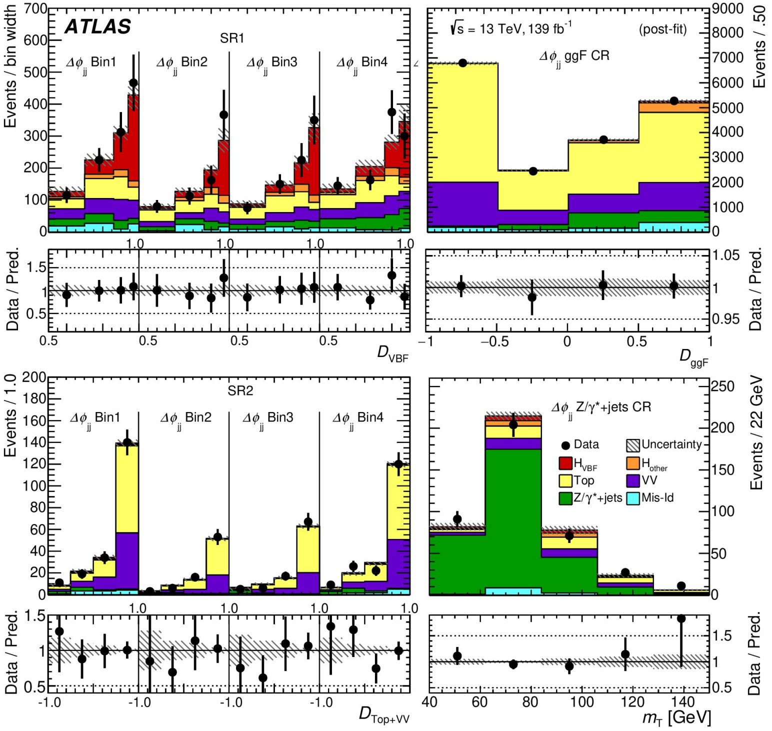

PRD 108 (2023) 072003

VBF, $H \to WW^* \to e\nu\mu\nu$: fiducial phase space and observed uncertainties

Selection Requirements	Signal Region	Fiducial Region
Lepton pair flavors	e-μ	e-μ
Lepton pair charge	0	0
Leading (subleading) lepton p_{T}	> 22 GeV (> 15 GeV)	> 22 GeV (> 15 GeV)
Lepton η^{ℓ}	$\lvert\eta^{\mu}\rvert < 2.5$ $0 < \lvert\eta^{e}\rvert < 1.37$ or $1.52 < \lvert\eta^{e}\rvert < 2.47$	$\lvert\eta^{\mu}\rvert < 2.5$ $\lvert\eta^{e}\rvert < 2.5$
No. of additional leptons	0	0
$\Delta R(\ell, \ell)$	overlap removal	> 0.1
$m_{\ell\ell}$	> 10 GeV	> 10 GeV
$\Delta R(\ell, \mathrm{jet})$	overlap removal	> 0.4
No. of jets ($p_{\mathrm{T}} > 30$ GeV, $\lvert\eta\rvert < 4.5$)	≥ 2	≥ 2
No. of b-jets ($p_{\mathrm{T}} > 20$ GeV, $\lvert\eta\rvert < 2.5$)	0	0
$m_{\tau\tau}$	$< m_Z - 25$ GeV	$< m_Z - 25$ GeV
Central jet veto ($p_{\mathrm{T}} > 20$ GeV)	✓	✓
Outside lepton veto	✓	✓
m_{jj}	> 450 GeV	> 450 GeV
$\lvert\Delta y_{jj}\rvert$	> 2.1	> 2.1
$\lvert\Delta\phi_{\ell\ell}\rvert$	< 1.4 rad	< 1.4 rad

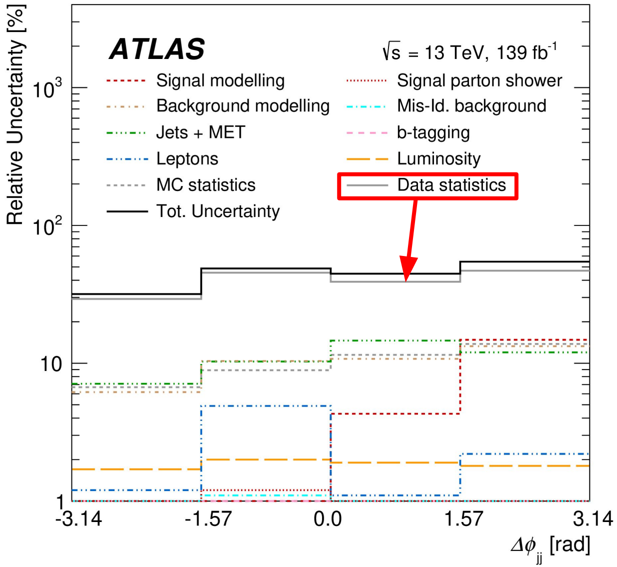

PRD 108 (2023) 072003

VBF, $H \to WW^* \to e\nu\mu\nu$: observed limits on dim-6 couplings

PRD 108 (2023) 072003

TABLE V. Summary of EFT operators in the SMEFT formalism that are probed with differential cross section measurements in the VBF $H \to WW^* \to e\nu\mu\nu$ channel. The corresponding structure in terms of the SM fields in the Warsaw basis (second column) is shown together with the associated Wilson coefficient (first column). The Higgs boson doublet field H and its complex conjugate are denoted by H and $H^\dagger$, respectively. The left-handed quark doublets (the right-handed up-type or down-type quarks) are denoted by q (u or d), while $V_{\mu\nu}$ ($\tilde{V}_{\mu\nu} = \epsilon^{\mu\nu\rho\sigma} V_{\rho\sigma}$) is the (dual) field strength tensor for a given gauge field of the electroweak interactions with $V = B, W^n$ ($n = \{1, 2, 3\}$), and τ^n are the Pauli matrices. The bosonic operators with (without) a dual field strength tensor are CP-odd (CP-even). For details of the formalism used see Ref. [128]. The expected and observed 95% confidence interval for the Wilson coefficients, using fits to the differential cross section measured as a function of the observable that is indicated in the 3rd column (labeled as "Fit distr"), are shown in the 5th and 6th columns, respectively. Results are presented when excluding (lin) or including (lin + quad) the pure dimension-six contributions to the EFT prediction, as indicated in the 4th column.

				95% Confidence interval [TeV^{-2}]	
Wilson coefficients	Operator structure	Fit distr	Paramater order	Expected	Observed
c_{HW}	$H^\dagger H W^n_{\mu\nu} W^{n\mu\nu}$	$\Delta\phi_{jj}$	lin	[−1.7, 1.6]	[−2.6, 0.60]
			lin + quad	[−1.4, 1.4]	[−1.8, 0.61]
c_{HB}	$H^\dagger H B_{\mu\nu} B^{\mu\nu}$	$\Delta\phi_{jj}$	lin	[−5.9, 6.4]	[−6.7, 4.6]
			lin + quad	[−0.59, 0.66]	[−0.60, 0.66]
c_{HWB}	$H^\dagger \tau^n H W^n_{\mu\nu} B^{\mu\nu}$	$\Delta\phi_{jj}$	lin	[−10, 9]	[−14, 5.9]
			lin + quad	[−1.2, 1.1]	[−1.2, 1.1]
c_{Hq1}	$(H^\dagger i\overleftrightarrow{D}_\mu H)(\bar{q}\gamma^\mu q)$	p_T^{j1}	lin	[−12, 15]	[−6.9, 22]
			lin + quad	[−1.9, 1.7]	[−2.2, 2.0]
c_{Hq3}	$(H^\dagger i\overleftrightarrow{D}^n_\mu H)(\bar{q}\tau^n\gamma^\mu q)$	p_T^{j1}	lin	[−0.56, 0.47]	[−0.74, 0.30]
			lin + quad	[−0.43, 1.2]	[−0.56, 0.43]
c_{Hu}	$(H^\dagger i\overleftrightarrow{D}_\mu H)(\bar{u}\gamma^\mu u)$	p_T^{j1}	lin	[−8.3, 6.9]	[-11, 4.2]
			lin + quad	[−2.0, 2.6]	[−2.5, 3.1]
c_{Hd}	$(H^\dagger i\overleftrightarrow{D}_\mu H)(\bar{d}\gamma^\mu d)$	p_T^{j1}	lin	[−21, 25]	[−13, 33]
			lin + quad	[−3.0, 2.7]	[−3.7, 3.4]
$c_{H\tilde{W}}$	$H^\dagger H \tilde{W}^n_{\mu\nu} W^{n\mu\nu}$	$\Delta\phi_{jj}$	lin	[−1.7, 1.7]	[−1.8, 1.3]
			lin + quad	[−1.4, 1.4]	[−1.6, 1.2]
$c_{H\tilde{B}}$	$H^\dagger H \tilde{B}_{\mu\nu} B^{\mu\nu}$	$\Delta\phi_{jj}$	lin	[−28, 28]	[−32, 22]
			lin + quad	[−0.62, 0.62]	[−0.63, 0.63]
$c_{H\tilde{W}B}$	$H^\dagger \tau^n H \tilde{W}^n_{\mu\nu} B^{\mu\nu}$	$\Delta\phi_{jj}$	lin	[−15, 15]	[−17, 12]
			lin + quad	[−1.2, 1.1]	[−1.2, 1.1]

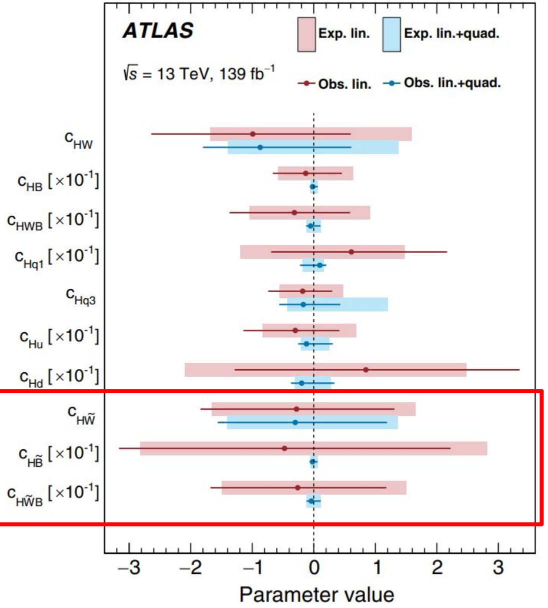

$H \rightarrow \tau\tau$: SR selections and sensitivity categorization

EPJC 83 (2023) 563

VBF		Boost	
$p_T^{j_2} > 30$ GeV $m_{jj} > 400$ GeV $\lvert\Delta\eta_{jj}\rvert > 3.0$ $\eta_{j_1} \cdot \eta_{j_2} < 0$ Central τ-leptons		Not VBF $p_T^{\tau\tau} > 100$ GeV	
Signal region ($110 < m_{\tau\tau}^{\mathrm{MMC}} < 150$ GeV)			
VBF_1	VBF_0	Boost_1	Boost_0
BDT(VBF) > 0	BDT(VBF) < 0	$\Delta R_{\tau\tau} < 1.5$ and $p_T^{\tau\tau} > 140$ GeV	$\Delta R_{\tau\tau} > 1.5$ or $p_T^{\tau\tau} < 140$ GeV
$Z \rightarrow \tau\tau$ control region ($60 < m_{\tau\tau}^{\mathrm{MMC}} < 110$ GeV)			
VBF_1 Z CR	VBF_0 Z CR	Boost_1 Z CR	Boost_0 Z CR

MMC ≔ missing mass calculator

Channel	Signal region	Decay mode combination	Selection criteria
$\tau_{\mathrm{lep}}\tau_{\mathrm{had}}$	High	ℓ–1p0n	$\lvert d_0^{\mathrm{sig}}(e)\rvert > 2.5$ or $\lvert d_0^{\mathrm{sig}}(\mu)\rvert > 2.0$ $\lvert d_0^{\mathrm{sig}}(\tau_{1\mathrm{p0n}})\rvert > 1.5$
		ℓ–1p1n	$\lvert d_0^{\mathrm{sig}}(e)\rvert > 2.5$ or $\lvert d_0^{\mathrm{sig}}(\mu)\rvert > 2.0$ $\lvert y^{\rho}(\tau_{1\mathrm{p1n}})\rvert > 0.1$
	Medium	ℓ–1pXn	$\lvert d_0^{\mathrm{sig}}(e)\rvert > 2.5$ or $\lvert d_0^{\mathrm{sig}}(\mu)\rvert > 2.0$ $\lvert y^{\rho}(\tau_{1\mathrm{pXn}})\rvert > 0.1$
		ℓ–3p0n	$\lvert d_0^{\mathrm{sig}}(e)\rvert > 2.5$ or $\lvert d_0^{\mathrm{sig}}(\mu)\rvert > 2.0$ $\lvert y^{a_1}(\tau_{3\mathrm{p0n}})\rvert > 0.6$
	Low	All above	Not satisfying selection criteria

Channel	Signal region	Decay mode combination	Selection criteria
$\tau_{\mathrm{had}}\tau_{\mathrm{had}}$	High	1p0n–1p0n	$\lvert d_0^{\mathrm{sig}}(\tau_1)\rvert > 1.5$ $\lvert d_0^{\mathrm{sig}}(\tau_2)\rvert > 1.5$
		1p0n–1p1n	$\lvert d_0^{\mathrm{sig}}(\tau_{1\mathrm{p0n}})\rvert > 1.5$ $\lvert y^{\rho}(\tau_{1\mathrm{p1n}})\rvert > 0.1$
		1p1n–1p1n	$\lvert y^{\rho}(\tau_1)y^{\rho}(\tau_2)\rvert > 0.2$
	Medium	1p0n–1pXn	$\lvert d_0^{\mathrm{sig}}(\tau_{1\mathrm{p0n}})\rvert > 1.5$ $\lvert y^{\rho}(\tau_{1\mathrm{pXn}})\rvert > 0.1$
		1p1n–1pXn	$\lvert y^{\rho}(\tau_{1\mathrm{p1n}})y^{\rho}(\tau_{1\mathrm{pXn}})\rvert > 0.2$
		1p1n–3p0n	$\lvert y^{\rho}(\tau_{1\mathrm{p1n}})\rvert > 0.1$ $\lvert y^{a_1}(\tau_{3\mathrm{p0n}})\rvert > 0.6$
	Low	All above	Not satisfying selection criteria

$H\to\tau\tau$: post-fit results

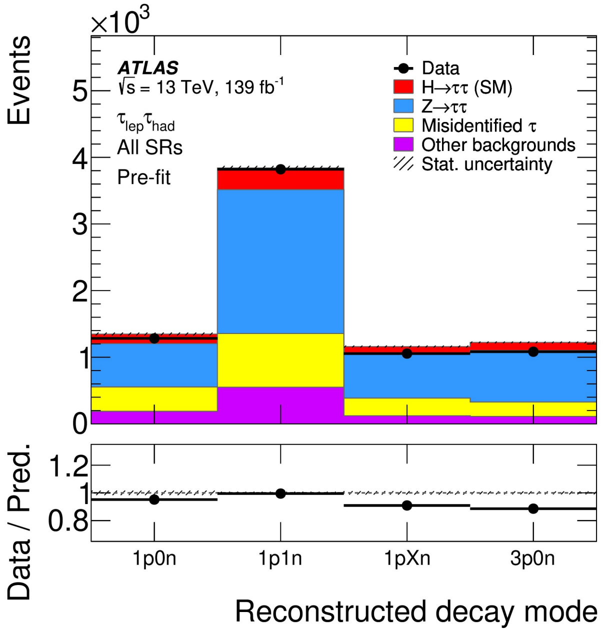

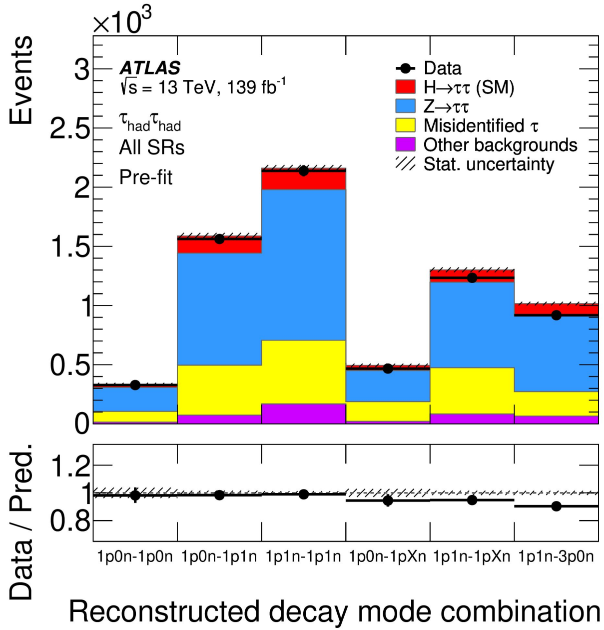

EPJC 83 (2023) 563

Fitted parameters	Observed	Expected
ϕ_τ	$9° \pm 16°$	$0° \pm 28°$
$\mu_{\tau\tau}$	$1.02^{+0.20}_{-0.20}$	$1.00^{+0.21}_{-0.21}$
$\mathrm{NF}^{\mathrm{Boost\_1}}_{Z\to\tau\tau}$	1.01 ± 0.05	1.00 ± 0.04
$\mathrm{NF}^{\mathrm{Boost\_0}}_{Z\to\tau\tau}$	1.02 ± 0.05	1.00 ± 0.05
$\mathrm{NF}^{\mathrm{VBF\_1}}_{Z\to\tau\tau}$	1.04 ± 0.08	1.00 ± 0.08
$\mathrm{NF}^{\mathrm{VBF\_0}}_{Z\to\tau\tau}$	0.95 ± 0.07	1.00 ± 0.08

$H \rightarrow \tau\tau$: observed uncertainties

Set of nuisance parameters	Impact on ϕ_τ [degrees]
Jet energy scale	3.4
Jet energy resolution	2.5
Pile-up jet tagging	0.5
Jet flavour tagging	0.2
E_T^{miss}	0.4
Electron	0.3
Muon	0.9
τ_{had} reconstruction	1.0
Misidentified τ	0.6
τ_{had} decay mode classification	0.3
π^0 angular resolution and energy scale	0.2
Track ($\pi^\pm$, impact parameter)	0.7
Luminosity	0.1
Theory uncertainty in $H \rightarrow \tau\tau$ processes	1.5
Theory uncertainty in $Z \rightarrow \tau\tau$ processes	1.1
Simulated background sample statistics	1.4
Signal normalisation	1.4
Background normalisation	0.6
Total systematic uncertainty	5.2
Data sample statistics	15.6
Total	16.4

EPJC 83 (2023) 563

$ttH+tH$, $H\rightarrow bb$: region definitions and observables

Training regions (TRs) broadly contain signal and are used to train multivariate algorithms

Region		Dilepton				ℓ+jets			
		$\mathrm{TR}^{\geq 4j,\geq 4b}$	$\mathrm{CR}_{\mathrm{hi}}^{\geq 4j,3b}$	$\mathrm{CR}_{\mathrm{lo}}^{\geq 4j,3b}$	$\mathrm{CR}_{\mathrm{hi}}^{3j,3b}$	$\mathrm{TR}^{\geq 6j,\geq 4b}$	$\mathrm{CR}_{\mathrm{hi}}^{5j,\geq 4b}$	$\mathrm{CR}_{\mathrm{lo}}^{5j,\geq 4b}$	$\mathrm{TR}_{\mathrm{boosted}}$
N_{jets}		≥ 4			$= 3$	≥ 6	$= 5$		≥ 4
$N_{b\text{-tag}}$	@85%	–				≥ 4			
	@77%	–				–			$\geq 2^{\dagger}$
	@70%	≥ 4	$= 3$			≥ 4			–
	@60%	–	$= 3$	< 3	$= 3$	–	≥ 4	< 4	–
$N_{\text{boosted cand.}}$		–				0			≥ 1
Fit observable		–	Yield			–	$\Delta R_{bb}^{\mathrm{avg}}$		–

Channel (TR)	Final SRs and CRs	Classification BDT selection	Fitted observable
Dilepton ($\mathrm{TR}^{\geq 4j,\geq 4b}$)	$\mathrm{CR}_{\text{no-reco}}^{\geq 4j,\geq 4b}$	–	$\Delta\eta_{\ell\ell}$
	$\mathrm{CR}^{\geq 4j,\geq 4b}$	$\mathrm{BDT}^{\geq 4j,\geq 4b} \in [-1,-0.086)$	b_4
	$\mathrm{SR}_1^{\geq 4j,\geq 4b}$	$\mathrm{BDT}^{\geq 4j,\geq 4b} \in [-0.086, 0.186)$	b_4
	$\mathrm{SR}_2^{\geq 4j,\geq 4b}$	$\mathrm{BDT}^{\geq 4j,\geq 4b} \in [0.186, 1]$	b_4
ℓ+jets ($\mathrm{TR}^{\geq 6j,\geq 4b}$)	$\mathrm{CR}_1^{\geq 6j,\geq 4b}$	$\mathrm{BDT}^{\geq 6j,\geq 4b} \in [-1,-0.128)$	b_2
	$\mathrm{CR}_2^{\geq 6j,\geq 4b}$	$\mathrm{BDT}^{\geq 6j,\geq 4b} \in [-0.128, 0.249)$	b_2
	$\mathrm{SR}^{\geq 6j,\geq 4b}$	$\mathrm{BDT}^{\geq 6j,\geq 4b} \in [0.249, 1]$	b_2
ℓ+jets ($\mathrm{TR}_{\mathrm{boosted}}$)	$\mathrm{SR}_{\mathrm{boosted}}$	$\mathrm{BDT}^{\mathrm{boosted}} \in [-0.05, 1]$	$\mathrm{BDT}^{\mathrm{boosted}}$

CP-sensitive observables

PLB 849 (2024) 138469

ttH+tH, H→bb: post-fit yields

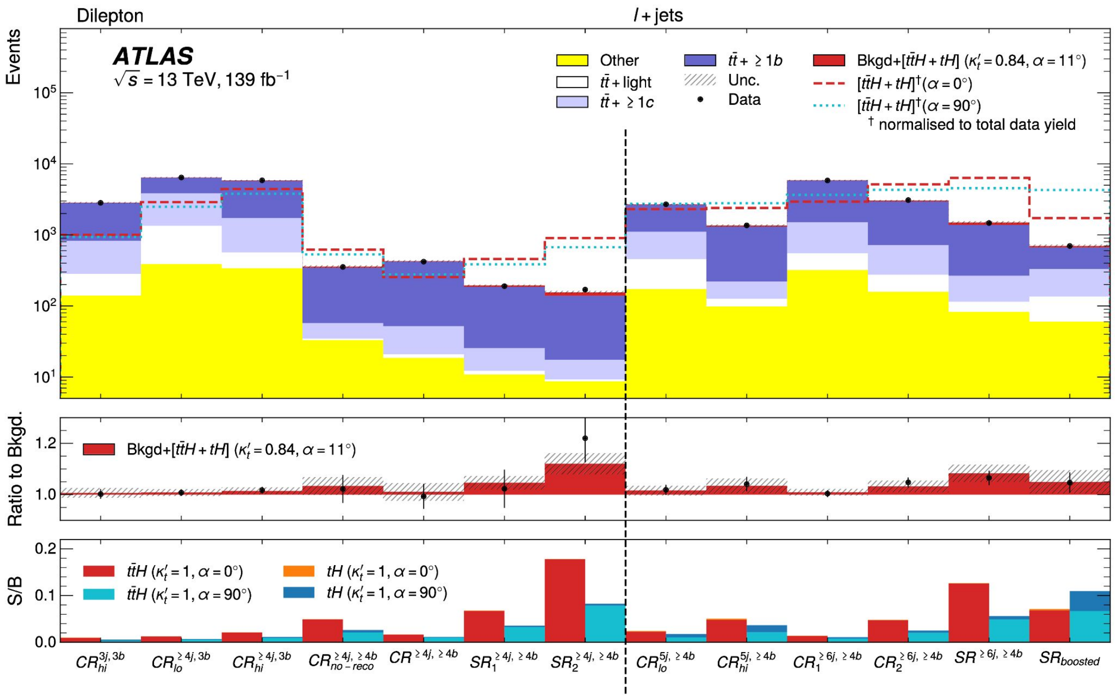

PLB 849 (2024) 138469

ttH+tH, $H\rightarrow bb$: observed uncertainties

Uncertainty source	$\Delta\alpha\,[^\circ]$	
Process modelling		
Signal modelling	+8.8	-14
$t\bar{t}+\geq 1b$ modelling		
$t\bar{t}+\geq 1b$ 4V5 FS	+23	-37
$t\bar{t}+\geq 1b$ NLO matching	+22	-33
$t\bar{t}+\geq 1b$ fractions	+14	-21
$t\bar{t}+\geq 1b$ FSR	+5.2	-9.9
$t\bar{t}+\geq 1b$ PS & hadronisation	+16	-24
$t\bar{t}+\geq 1b$ $p_T^{b\bar{b}}$ shape	+5.4	-4.6
$t\bar{t}+\geq 1b$ ISR	+14	-24
$t\bar{t}+\geq 1c$ modelling	+6.6	-11
$t\bar{t}$ + light modelling	+2.5	-4.7
b-tagging efficiency and mis-tag rates		
b-tagging efficiency	+8.7	-15
c-mis-tag rates	+6.7	-11
l-mis-tag rates	+2.3	-2.7
Jet energy scale and resolution		
b-jet energy scale	+1.6	-3.8
Jet energy scale (flavour)	+7.8	-11
Jet energy scale (pileup)	+5.2	-7.9
Jet energy scale (remaining)	+8.1	-13
Jet energy resolution	+5.7	-9.3
Luminosity	$\leq \pm 1$	
Other sources	+4.9	-8
Total systematic uncertainty	+41	-54
$t\bar{t}+\geq 1b$ normalisation	+8.2	-13
κ_t'	+17	-33
Total statistical uncertainty	+32	-49
Total uncertainty	+52	-73

Uncertainty source	$\Delta\kappa_t'$	
Process modelling		
Signal modelling	+0.10	-0.10
$t\bar{t}+\geq 1b$ modelling		
$t\bar{t}+\geq 1b$ 4V5 FS	+0.08	-0.23
$t\bar{t}+\geq 1b$ NLO matching	+0.15	-0.30
$t\bar{t}+\geq 1b$ fractions	+0.09	-0.21
$t\bar{t}+\geq 1b$ FSR	+0.01	-0.02
$t\bar{t}+\geq 1b$ PS & hadronisation	+0.09	-0.20
$t\bar{t}+\geq 1b$ $p_T^{b\bar{b}}$ shape	+0.07	-0.11
$t\bar{t}+\geq 1b$ ISR	+0.07	-0.17
$t\bar{t}+\geq 1c$ modelling	+0.04	-0.10
$t\bar{t}$ + light modelling	+0.00	-0.01
b-tagging efficiency and mis-tag rates		
b-tagging efficiency	+0.06	-0.12
c-mis-tag rates	+0.03	-0.07
l-mis-tag rates	+0.01	-0.03
Jet energy scale and resolution		
b-jet energy scale	+0.02	-0.02
Jet energy scale (flavour)	+0.01	-0.05
Jet energy scale (pileup)	+0.02	-0.05
Jet energy scale (remaining)	+0.04	-0.08
Jet energy resolution	+0.03	-0.09
Luminosity	$\leq \pm 0.01$	
Other sources	+0.03	-0.07
Total systematic uncertainty	+0.29	-0.45
$t\bar{t}+\geq 1b$ normalisation	+0.05	-0.15
α	+0.08	-0.07
Total statistical uncertainty	+0.09	-0.10
Total uncertainty	+0.30	-0.46

PLB 849 (2024) 138469